

# Phase Modification of SEBS Block Copolymer by Different Additives and Its Effect on Morphology, Mechanical and Dynamic Mechanical Properties

SUBIMAN GHOSH, D. KHASTGIR, ANIL K. BHOWMICK

Rubber Technology Centre, Indian Institute of Technology, Kharagpur 721302, India

Received 23 April 1997; accepted 19 August 1997

**ABSTRACT:** The objective of this study is to examine the phase modification of styrene–ethylene butylene–styrene (SEBS) block copolymer by different additives and its influence on morphology and mechanical, and dynamic mechanical properties. The additives chosen are the coumarone–indene (CI), phenol–formaldehyde (PF), paraffin hydrocarbon (PAHY) resins, as well as aromatic oil (AO), polystyrene (PS), polypropylene (PP), ethylene vinyl acetate (EVA) (VA 28 and 45%), and ethylene propylene diene monomer (EPDM) rubber. It is interesting to note that of all the additives, PP has the most prominent effect. The mechanical properties of SEBS polymer are enhanced to a large extent by PP. The value of  $\tan \delta$  maximum of SEBS at both the low and the high temperature transitions is decreased. All the resins and PS increase the storage modulus and the tensile modulus of the SEBS polymer. CI resin and AO modify the hard and soft phases of SEBS polymer. AO, EPDM rubber, and EVA lower the mechanical strength of the SEBS polymer. The results are explained on the basis of morphology studied with the help of scanning electron microscopy. © 1998 John Wiley & Sons, Inc. *J Appl Polym Sci* **67**: 2015–2025, 1998

**Key words:** SEBS; block copolymer; modification; morphology; dynamic mechanical properties; hysteresis; additives

## INTRODUCTION

Thermoplastic elastomers form a new class of polymeric materials that have large number of applications because of their unique combination of mechanical properties and processability. Their modulus level is comparable to that of the reinforced rubber vulcanizate at the use conditions, which cover the range from the low temperature near the glass transition temperature of the rubbery component to the higher temperature approaching the melting or softening point of the plastic component. At the processing temperature, they are in the melt state such that they can

be processed with plastic processing equipment. Among the thermoplastic elastomers, the triblock copolymer is a special kind. Typical examples are styrene–butadiene–styrene (SBS), styrene–isoprene–styrene (SIS), and styrene–ethylene butylene–styrene (SEBS) block copolymers.

The molecular structures can be tailor-made to have a narrow molecular weight distribution in each block, and their typical properties are due to the thermodynamic incompatibility of the two components in the solid state that leads to a microphase separation. Owing to this phenomenon, the material can be considered as an elastomeric matrix physically vulcanized by the aggregation of the polystyrene (PS) end blocks in spherical domains, which also act as reinforcing filler. Usually, polystyrene is a minor component and has spherical domains at low concentration.

---

Correspondence to: A. K. Bhowmick.

*Journal of Applied Polymer Science*, Vol. 67, 2015–2025 (1998)  
© 1998 John Wiley & Sons, Inc. CCC 0021-8995/98/122015-11



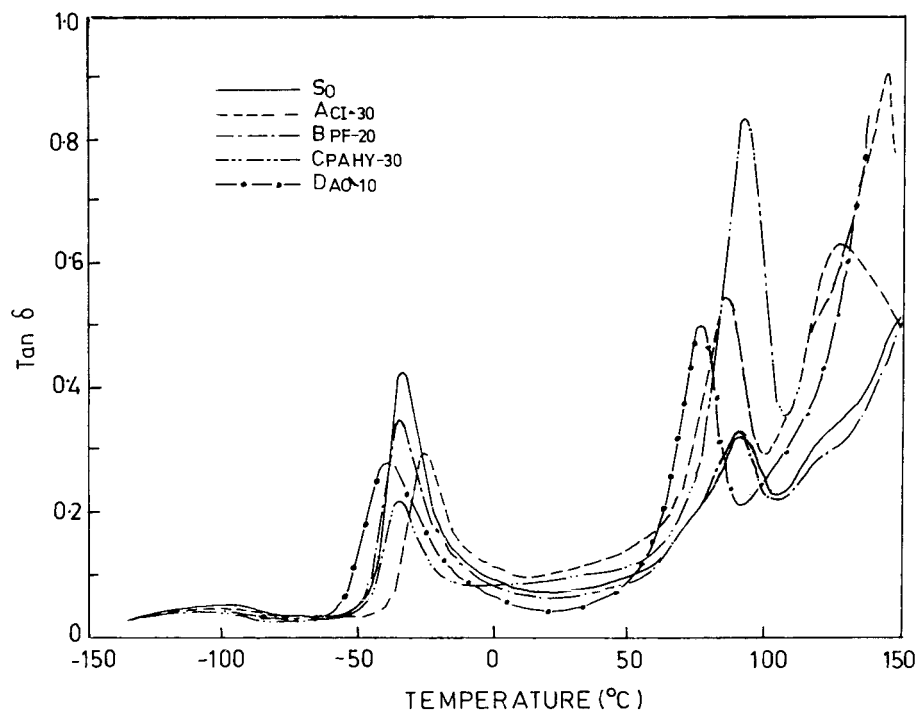


**Figure 1** Tan  $\delta$ -temperature curves for control and CI resin, PF resin, PAHY resin, and AO-modified SEBS (frequency: 1 Hz).

obtained from Hind Plastics, Visakhapatnam, India. PP with specific gravity of 0.90 was obtained from I.P.C.L., Gujrat, India. Pilene EVA with a VA content of 28% (by weight) and specific gravity of 0.96 was obtained from Polyolefin Industries Ltd., Bombay, India. Livaprene 45 LX EVA with a VA content of 45% (by weight) and specific gravity 0.97 was obtained from Bayer India Ltd., Bombay, India. EPDM rubber, JSR-EP-96, with ethylene content of 55 mol %, diene (DCPD) content of 4.5 mol %, and a specific gravity of 0.86 was obtained from Japan Synthetic Rubber Company Ltd., Japan.

### Mixing and Molding

A complete list of mixes and their composition are given in Table I. The mixes were prepared in a Brabender Plasticorder (model PLE-330) using a cam type rotor, with a speed of 62 rpm and a mixer chamber temperature of 180°C. Initially, the SEBS block copolymer was melted in the mixer for 2 min, then the different additives were added to it and mixed for another 2 min. The mix was then taken out and sheeted through a laboratory mill at 25°C with the minimum nip gap ( $\sim 2.5$  mm). The sheeted out material was remixed in

the Plasticorder under similar conditions for 2 min to ensure uniform dispersion of the additives and homogeneity of the mix and finally sheeted out through the two-roll mill.

The sheeted-out stock was compression-molded between the aluminium foils in a Moore press at 190°C for 5 min at 5 MPa pressure to give sheets of 2.0 mm thickness. At the end of the molding time, the sample still under compression was cooled by circulating water at room temperature through the platens until the temperature dropped to 50°C. Aluminium foils were used between the mold surface to reduce shrink marks on the sheet.

### Dynamic Property Measurements

Dynamic mechanical properties under bending mode were evaluated using DMTA (model No. MK-II, Polymer Laboratories, U.K.). The frequencies selected were 0.01, 0.1, 1, and 10 Hz, though the data at 1 Hz were reported in this article. A double strain amplitude of 64  $\mu\text{m}$  was used. The experiments were carried out from  $-130^\circ\text{C}$  to  $+150^\circ\text{C}$  at the heating rate of  $2^\circ\text{C}/\text{min}$ . The data was recorded and analyzed by a COMPAQ computer.

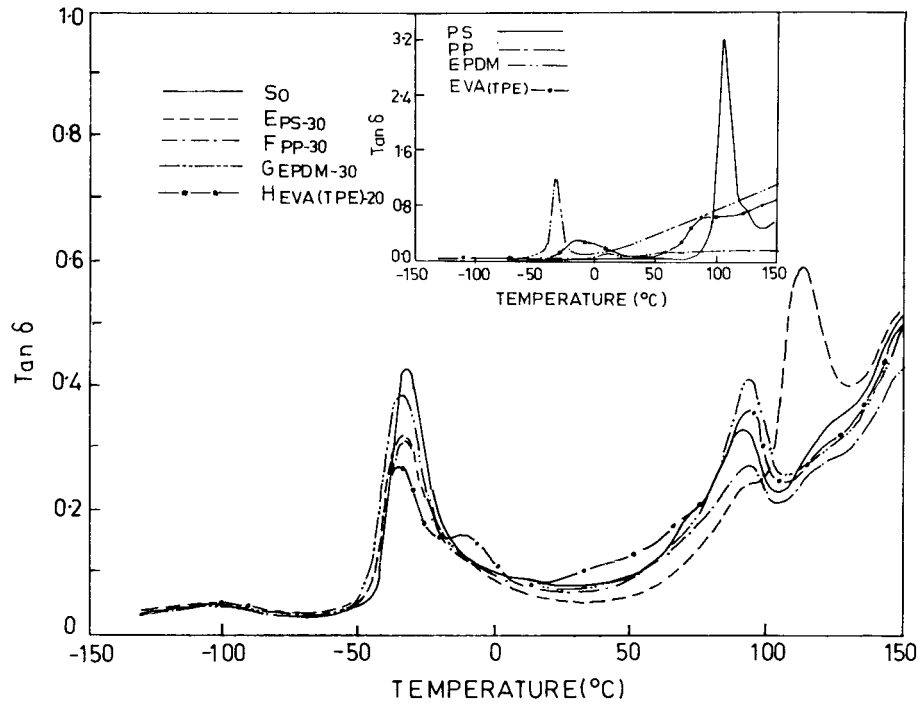


**Figure 2** Tan  $\delta$ -temperature curves for control and PS, PP, EPDM, EVA<sub>TPE</sub>, modified SEBS (frequency: 1 Hz). Inset: tan  $\delta$ -temperature curves for PS, PP, EPDM, and EVA<sub>TPE</sub> (frequency: 1 Hz).

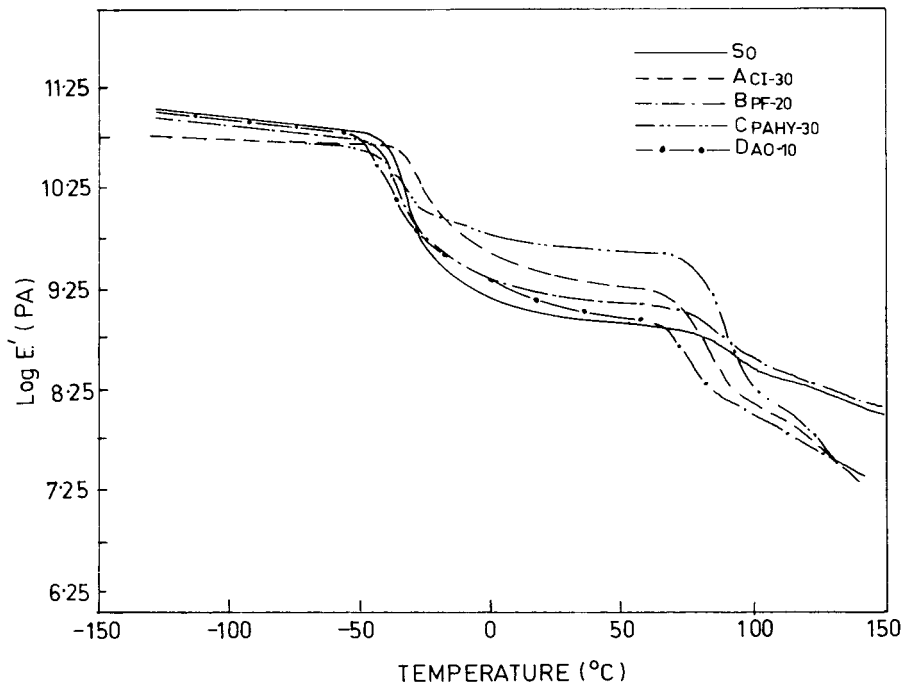


**Figure 3** Storage modulus-temperature curves for control and CI resin, PF resin, PAHY resin, and AO-modified SEBS (frequency: 1 Hz).

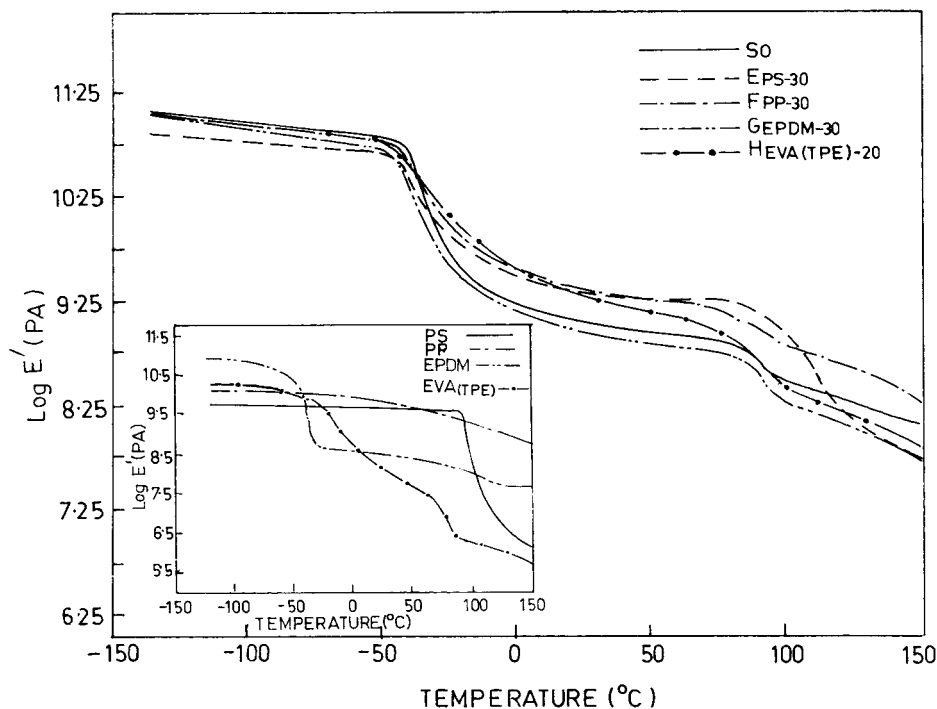


**Figure 4** Storage modulus–temperature curves for control and PS, PP, EPDM, and EVA<sub>TPE</sub>-modified SEBS (frequency: 1 Hz). Inset: storage modulus–temperature curves for PS, PP, EPDM, and EVA<sub>TPE</sub> (frequency: 1 Hz).

**Tensile Testing**

Tensile strength, modulus, and elongation at break were measured as per ASTM D412-80 in a computerized Zwick UTM (1445) at a crosshead speed of 500 mm/min. The dumbbell-shaped specimens were obtained from the molded sheets. The

results of six tests on each sample were averaged. An error of ±5% was recorded.

**Hysteresis Study**

Hysteresis was obtained on tensile dumbbell specimen at 100% elongation at loading and unloading

**Table II** Tanδ Peak Values and the Transition Temperatures of the Control and Modified SEBS

Mixed Compound	EB Transition		PS Transition	
	Tanδ Peak Value	Transition Temperature (°C)	Tanδ Peak Value	Transition Temperature (°C)
S <sub>0</sub>	0.435	-32.5	0.335	+91.5
A <sub>CI-30</sub>	0.286	-25	0.521	85
B <sub>PP-20</sub>	0.35	-34	0.345	90.5
C <sub>PAHY-30</sub>	0.225	-34	0.845	92
D <sub>AO-10</sub>	0.32	-38.5	0.535	76.5
E <sub>PS-30</sub>	0.32	-34	0.595	112.5
F <sub>PP-10</sub>	0.475	-36	0.25	91.5
F <sub>PP-20</sub>	0.455	-35	0.25	91.5
F <sub>PP-30</sub>	0.39	-32.5	0.275	92
G <sub>EPDM-30</sub>	0.295	-35	0.41	93.5
H <sub>EVA-R-20</sub>	0.33	-35.5	0.35	90
H <sub>EVA-TPE-20</sub>	0.275	-34.5	0.36	93.5

**Table III** Log  $E'$  Values of the Control and Modified SEBS

Mix Number	Log $E'$ of Glassy Region (Pa)	Log $E'$ of Rubbery Plateau (Pa)	Log $E'$ of Plastic Melting Zone (Pa)
S <sub>0</sub>	10.89–10.74	8.94–8.79	8.37–8.04
A <sub>CI-30</sub>	10.71–10.62	9.39–9.24	8.1–7.32
B <sub>PF-20</sub>	10.83–10.71	9.16–9.06	8.4–8.07
C <sub>PAHY-30</sub>	10.71–10.62	9.72–9.57	7.98–7.32
D <sub>AO-10</sub>	10.86–10.77	9.03–8.91	8.1–7.26
E <sub>PS-30</sub>	10.83–10.65	9.24–9.18	7.95–7.71
F <sub>PP-10</sub>	10.92–10.68	8.64–8.55	8.4–8.01
F <sub>PP-20</sub>	10.92–10.71	8.82–8.73	8.46–8.1
F <sub>PP-30</sub>	10.89–10.74	9.33–9.15	8.79–8.31
G <sub>EPDM-30</sub>	10.95–10.65	8.88–8.64	8.13–7.77
H <sub>EVA<sub>TPE</sub>20</sub>	10.89–10.77	9.39–9.03	8.25–7.83
H <sub>EVA<sub>R</sub>20</sub>	10.92–10.65	9.0–8.91	8.07–7.74

rates of 500 mm/min at 25°C. The hysteresis ratio ( $H_R$ ) was calculated using the following formulae:

$$H_R = \frac{W_E - W_R}{W_E} = \frac{\Delta W}{W_E} \quad (1)$$

where  $W_E$  represents the work done during extension, and  $W_R$  represents the work done during retraction. The tensile set was also determined from this experiment. Six samples were tested for each value reported in this article.

### Morphology Study

Surface morphology of the mixes was studied by scanning electron microscopy (SEM) (Cam Scan Series-II model). One of the phases was extracted with a solvent, and the samples were dried and sputter-coated with gold before examination.

### Solvent Extraction Study

Acetone was used to extract out CI resin from SEBS–CI mix, while methyl ethyl ketone was chosen for extracting paraffin hydrocarbon resin from the SEBS–PAHY mix. SEBS was extracted out from the mixture of SEBS–PP with the help of cyclohexane solvent.

## RESULTS AND DISCUSSION

### Dynamic Mechanical Properties

Dynamic mechanical properties of the control SEBS and SEBS mixed with other additives are

reported in Figures 1–4. The data are recorded in Tables II and III.

SEBS displays the following three transition peaks: the first near  $-105^\circ\text{C}$ , due to the cooperative movement of the methylene groups of the ethylene butylene segments; the second at  $-32.5^\circ\text{C}$ , due to the relaxation of the soft elastomeric ethylene–butylene segments; and the third at  $+91.5^\circ\text{C}$ , due to the relaxation of the hard PS domains (Fig. 1). The values of  $\tan \delta$  peaks at  $-32.5^\circ\text{C}$  and  $91.5^\circ\text{C}$  are 0.435 and 0.335, respectively (Table II). The range of log  $E'$  values in the plateau zone at  $26$ – $69^\circ\text{C}$  is  $8.94$ – $8.79$  Pa (Table III). In subsequent discussion, the peaks at  $-32.5$  and  $+91.5^\circ\text{C}$  will be discussed, as there is no significant change of the peak at  $-105^\circ\text{C}$  ( $\tan \delta_{\max} = 0.05$ ) with the incorporation of the additives.

From Table II, it is observed that all the additives (except PP at low concentration) when added to SEBS decrease its  $\tan \delta$  peak at the lower transition region but increase the  $\tan \delta$  peak at the upper transition region. The changes in the  $\tan \delta$  peak values at the upper and lower transition regions are the opposite for PP up to 20 phr. Similarly, all the additives except CI resin and 30 phr PP decrease the lower transition temperature of SEBS (Table II). The CI resin increases the lower transition temperature, while, for PP, the temperature remains unaltered. It may be noted that glass transition temperature of PP occurs at  $13^\circ\text{C}$  with a  $\tan \delta_{\max}$  of 0.10.

The CI resin, PF resin, AO, and EVA<sub>R</sub> decrease the upper transition temperature of SEBS, while PS, EPDM, and EVA<sub>TPE</sub> increase it (Table II). The PAHY resin and PP do not alter the upper

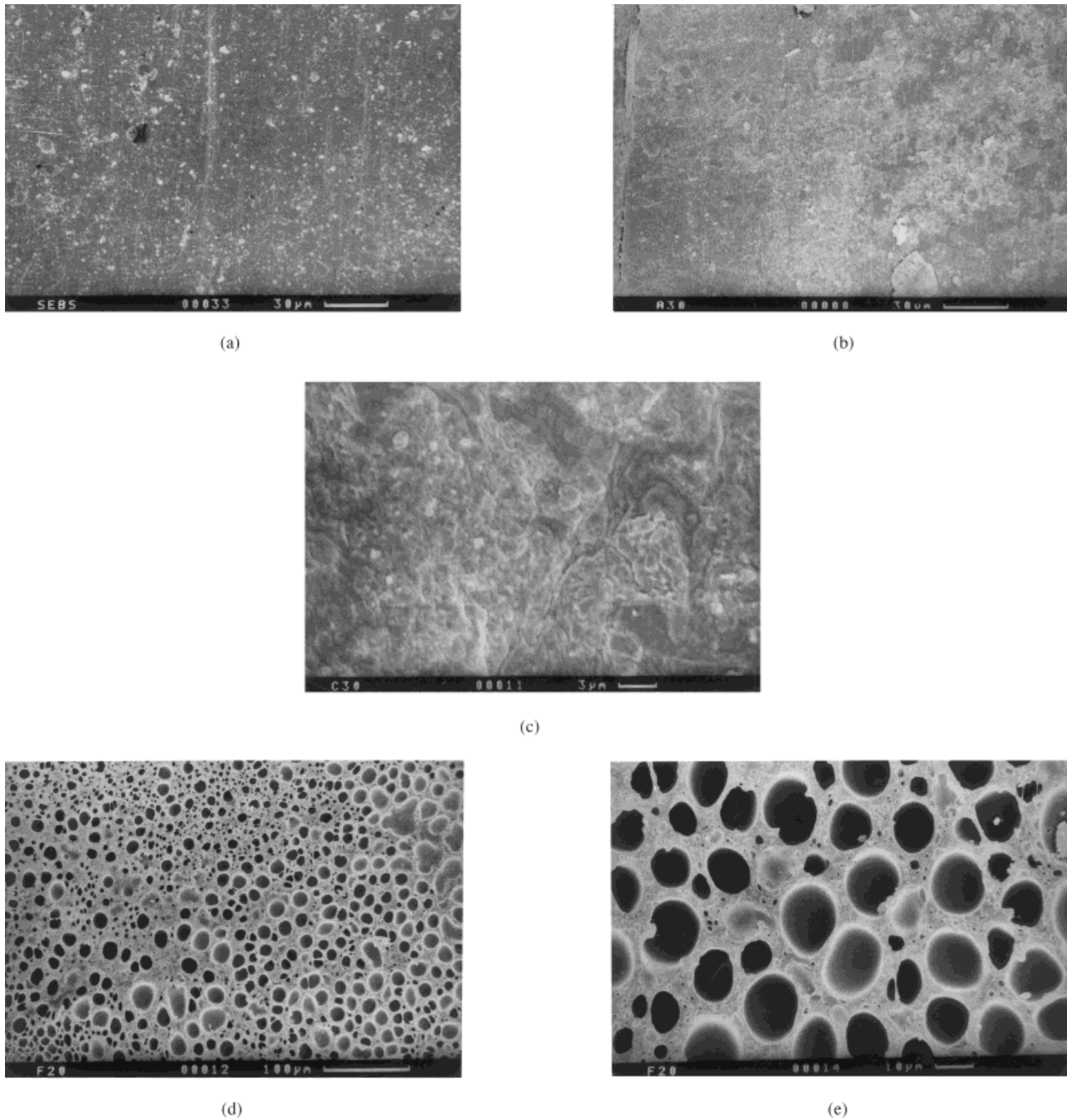


**Figure 5** SEM micrographs of some representative mixes: (a) surface photograph of control SEBS; (b) surface photograph of  $A_{CI-30}$  mix, where CI resin was extracted out with acetone; (c) surface photograph of  $C_{PAHY-30}$  mix, where PAHY resin was extracted out with methyl ethyl ketone solvent; (d) surface photograph of  $F_{PP-20}$  mix, where SEBS was extracted out with cyclohexane solvent; and (e) enlarged image of (d).

transition temperature of SEBS. It is interesting to note that all the additives except EPDM and PP at low concentrations increase the storage modulus and  $\log E'$  value of SEBS at the rubbery plateau zone (Table III). The  $E'$  value at the

glassy region is of the same order in each case. On the other hand, all the additives except PP and PF resin decrease the  $\log E'$  value of SEBS at the plastic melting zone. On comparison of 10, 20, and 30 phr PP-loaded SEBS, it is observed

that the  $\tan \delta$  peak of the respective mixes at the lower transition region decreases gradually, but the one at higher transition region remains almost the same. The lower transition temperature increases gradually in this case, but the upper transition temperature remains almost the same (Table II). With increasing PP loading, the  $\log E'$  value of the respective mixes at the rubbery plateau zone gradually increases, having the highest storage modulus (9.33–9.15 Pa) value at 30 phr loading of PP (Table III).

Findings of dynamic mechanical studies may be explained in the following lines. All the additives except the aromatic oil are glassy material at  $-32.5^\circ\text{C}$ . The external additives may reside in the soft phase, hard phase, or in both the phases, or it may form a separate third phase. It is possible that a part of the resins (CI, PF, and PAHY) may locate themselves amongst the soft EB segments, thereby resulting in the chain stiffening and hardening of the final product. This is reflected in the decrease of  $\tan \delta$  peak at  $-32.5^\circ\text{C}$  and the increase in  $\log E'$  value at the plateau region for the mixes. The resins, however, do not crosslink with the EB segments of SEBS polymer. The resins or SEBS could be extracted out from the resin–SEBS mixture by an appropriate solvent. An aromatic oil would swell the EB matrix of SEBS and also become solubilized in the PS microdomains. This would lead to a decrease in the glass transition temperature of both the phases and a displacement of the corresponding loss peaks to lower temperatures (Fig. 1).

The CI and PAHY resins have melting points of  $90$  and  $85^\circ\text{C}$ , respectively, which are lower than the softening point of the PS domains ( $105^\circ\text{C}$ ) of SEBS polymer. The melting of these resins near the upper transition region of SEBS makes the SEBS–resin mixture softer than the control SEBS, which is reflected in the increase of  $\tan \delta$  peak at the upper transition region (Fig. 1). For PF resin with a melting point of  $120^\circ\text{C}$ , there is no such softening effect on SEBS, so the  $\tan \delta$  peak max at  $91.5^\circ\text{C}$  remains almost the same. AO plasticizes the hard PS domains of SEBS, thereby making the material more soft; this increases the  $\tan \delta$  peak at  $91.5^\circ\text{C}$ . The external addition of PS to SEBS indicates the presence of a transition in the PS microdomains at the same temperature as the pure SEBS and a large separate PS transition at a considerably higher temperature ( $112.5^\circ\text{C}$  instead of  $91.5^\circ\text{C}$ ). It is quite possible that added PS is unable to enter the small PS microphase domains and mainly serves as a filler.

PP has a melting point of  $165^\circ\text{C}$ , which is higher than the softening point of PS domains. So the SEBS–PP mix is relatively more rigid than the control SEBS near the upper transition region, resulting in a decrease of  $\tan \delta$  peak (Fig. 2). EPDM, itself being an elastomer ( $T_g = -31^\circ\text{C}$ ;  $\tan \delta_{\text{max}} = 1.2$ ), enhances the elastomeric nature of SEBS–EPDM mix, which results in a softer material than control SEBS. This is reflected in the increase of  $\tan \delta$  peak at the upper transition zone. EVA has virtually no interaction with the PS domains, as evidenced by the fact that the  $\tan \delta$  peak at the upper transition region increases marginally in SEBS–EVA<sub>TPE</sub> mix. The small hump occurring at  $-12^\circ\text{C}$  is indicative of phase-separated EVA<sub>TPE</sub> (Fig. 2), as the glass transition temperature for pure EVA<sub>TPE</sub> measured under the same conditions is  $-13^\circ\text{C}$  ( $\tan \delta_{\text{max}} = 0.33$ ).

In order to understand the dilution effect of SEBS by various additives, we have analyzed the storage modulus curves by taking the volume fraction of the polymer ( $V_p$ ) into consideration. For example, the following relationship is found to hold for rubber–resin systems<sup>12</sup>:

$$G' = (V_p)^n G_o$$

where  $G'$  and  $G_o$  are the plateau modulus of the rubber–resin mixture and pure polymer, respectively. In the SEBS–resin systems, the value of  $n$  is found to be negative and lies between  $-0.3$  to  $-0.13$ , corresponding to range of  $V_p$  values of  $0.75$ – $0.91$ . With the increasing loading of the resin, the value of  $n$  remains constant. For  $A_{\text{CI}}$ ,  $B_{\text{PF}}$ ,  $C_{\text{PAHY}}$ , and  $D_{\text{AO}}$  mixes, the values of  $n$  are  $-0.19$ ,  $-0.14$ ,  $-0.30$ , and  $-0.13$ , respectively.

### Morphology Study

The SEM micrographs of the various mixes have been analyzed. Representative photographs of the mixes  $S_0$ ,  $A_{\text{CI-30}}$ ,  $C_{\text{PAHY-30}}$ , and  $F_{\text{PP-20}}$  are shown in Figure 5. It is observed that all the mixes except  $F_{\text{PP-20}}$  show similar morphological structures after extraction with acetone and methyl ethyl ketone solvents. The additives CI resin and PAHY resin are randomly distributed in the SEBS matrix. However, the most interesting photographs obtained are those of  $F_{\text{PP-20}}$ , where SEBS has been extracted out with cyclohexane solvent. The photographs clearly represent that PP forms the continuous matrix while SEBS forms the dispersed phase. This structure is also predominant in mixes containing 30 phr PP. Based on the DMTA



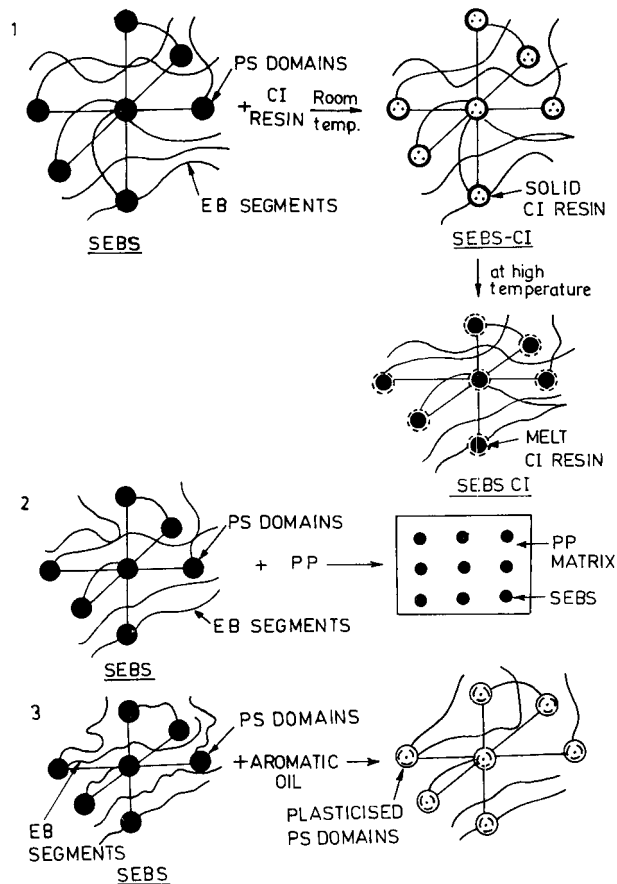
and SEM studies, the different types of interactions of SEBS with some of the additives can be envisaged as depicted in Scheme 1.

**Mechanical Properties**

The results of tensile testing are reported in Table IV and Figure 6, respectively. It is observed that the PF and PAHY resins, aromatic oil, polystyrene, EPDM, and EVA decrease the tensile strength (TS) of SEBS. The elongation at break ( $E_b$ ) is also lowered or remains constant except for a few cases. The modulus of SEBS displays a lower value when higher loadings of AO, EPDM, and EVA<sub>R</sub> have been added. The CI resin registers the maximum increase in elongation at break of SEBS polymer at 30 phr loading. With the increase in the loading of the resin, the tensile strength increases, but the modulus value registers an increase up to 20 phr loading for the same mix. However, the best results are obtained with PP, where there is 22% increase in tensile strength with 30 phr loading of PP. The modulus value also increases by 75%. The elongation at break increases from 708% in the case of control SEBS to 724% for 30 phr PP-loaded SEBS.

The results could be explained with the help of morphological structures and interaction between the additives and SEBS. PP forming the continuous matrix in  $F_{PP-20}$  is expected to show a high value of tensile strength and modulus as the strength of PP is higher than that of PS or EB. The increased modulus is also a result of the structure. Though the morphological structure in other cases is similar, the interaction between SEBS and other additives varies.

As discussed in the earlier section, the addition of 30 phr CI resin to SEBS causes a shift in the lower as well as the upper transition temperature of the base polymer (Table II). This means that the CI resin is compatible to a certain degree with the hard PS domains as well as with the soft EB matrix of SEBS. As a result, the proportion of the resin in the EB and PS phases dictates the properties. At higher loading, the resin probably resides in the PS phase, increasing the modulus and tensile strength values. The modulus value of SEBS registers an increase, while the tensile strength and elongation at break decrease considerably with increased loading of PF resin and PAHY resin. Probably a portion of these additives may phase separate or locate themselves amongst the EB segments. These portions then act as stress concentrators or flaws and decrease the



**Scheme 1** Mechanisms showing the interaction of different additives with the hard and soft phases of SEBS polymer: 1) CI resin interacts with both the phases of SEBS polymer at room and higher temperatures; 2) interaction of PP with SEBS where PP forms the matrix, and SEBS is dispersed as domains; 3) plasticizing effect of AO on the hard PS domains of SEBS polymer.

tensile strength from 28.3 MPa in the case of control SEBS to 21.0 and 24.4 MPa in the case of 20 phr loading of the PF and PAHY resins, respectively. The elongation at break also decreases from 708% in the case of control SEBS to 644 and 601% for PF resin and PAHY resin, respectively, at 20 phr loading. But as the loading of the additives increases, the modulus increases. The additives, being rigid materials, impart stiffness to SEBS polymer and enhance the modulus of the system. The hard PS domains are mainly responsible for the high mechanical strength of SEBS polymer; and, when plasticized by the addition of 10 phr of aromatic oil to SEBS, the base polymer become softer, leading to a fall in the tensile strength, elongation at break, and modulus values. EPDM rubber, being elastomeric in nature

**Table IV Mechanical Properties of the Control and Modified SEBS**

Mixed Compound	TS (MPa)	$E_b$ (%)	Modulus (MPa)			Set (%)	$H_R$
			100%	200%	300%		
S <sub>0</sub>	28.3	708	2.2	3.7	6.0	8	0.47
A <sub>CI-5</sub>	26.8	671	3.0	4.6	6.8	9	0.52
A <sub>CI-10</sub>	27.7	683	3.2	4.8	7.0	12	0.55
A <sub>CI-20</sub>	29.0	697	4.6	6.0	7.9	11	0.59
A <sub>CI-30</sub>	31.1	795	2.3	3.2	5.2	18	0.64
B <sub>PF-20</sub>	21.0	644	3.5	5.1	7.4	11	0.50
C <sub>PAHY-5</sub>	26.0	661	2.7	4.2	6.9	12	0.53
C <sub>PAHY-10</sub>	25.1	668	4.0	6.0	9.0	13	0.56
C <sub>PAHY-20</sub>	24.4	601	5.5	7.7	10.2	11	0.59
C <sub>PAHY-30</sub>	21.4	585	5.2	7.5	10.3	12	0.67
D <sub>AO-5</sub>	15.6	632	2.5	4.0	6.0	9	0.39
D <sub>AO-10</sub>	10.5	573	2.0	3.1	4.8	8	0.33
E <sub>PS-10</sub>	23.1	568	3.5	6.2	9.2	9	0.50
E <sub>PS-20</sub>	22.1	510	4.3	8.2	12.3	12	0.54
E <sub>PS-30</sub>	20.5	507	5.3	9.6	13.5	15	0.57
F <sub>PP-10</sub>	29.1	672	3.1	4.9	7.3	11	0.52
F <sub>PP-20</sub>	31.1	684	4.5	6.3	9.0	12	0.56
F <sub>PP-30</sub>	34.4	724	5.8	7.8	10.5	16	0.62
G <sub>EPDM-10</sub>	21.2	712	2.8	4.0	6.0	10	0.39
G <sub>EPDM-20</sub>	18.3	727	2.5	3.6	5.4	12	0.34
G <sub>EPDM-30</sub>	11.7	726	2.0	2.9	4.2	13	0.14
H <sub>EVA<sub>TPE-20</sub></sub>	20.8	732	2.2	3.2	5.1	16	0.4
H <sub>EVA<sub>R-20</sub></sub>	12.5	663	1.7	2.6	4.1	12	0.37

TS is defined as tensile strength;  $E_b$ , elongation at break;  $H_R$ , hysteresis ratio.

when added to SEBS, makes the polymer softer and elastomeric in character. This leads to a fall in the tensile strength value from 28.3 MPa in the case of control SEBS to a value as low as 11.7 MPa for 30 phr loading of EPDM. At the same loading of EPDM, the elongation at break increases from 708 to 726%, but the modulus value decreases. The EVA polymer, being polar in nature, is incompatible with SEBS polymer and does not mix well with it, as confirmed from the SEM photographs. It simply acts as a diluent to SEBS polymer, whereby the tensile strength decreases and the elongation at break and modulus decrease or remain the same.

### Hysteresis Study

The hysteresis ratio  $H_R$  and percentage set values for all the mixes are reported in Table IV. The  $H_R$  value for control SEBS is 0.47, while the set is 8%. It is interesting to note that the CI, PAHY, and PF resins and PS and PP increase the value of the hysteresis ratio of SEBS polymer. On the other hand, EPDM, EVA, and AO decrease it.

However, except for  $D_{AO-10}$ , the set increases in each case. Incorporation of 30 phr of the PAHY resin increases the hysteresis ratio of the SEBS polymer by 43%. PP at 20 phr loading, in spite of being the continuous matrix, registers a hysteresis ratio value of 0.54. The maximum set observed is 18% with the use of 30 phr CI resin, which is much less than the requirement for the mixture to be classed as a thermoplastic elastomer. The  $F_{PP-30}$  and  $H_{EVA_{TPE-20}}$  mixes show a maximum set value of 16%. The increase in hysteresis ratio is due to the extra energy dissipative mechanism, introduced through the incorporation of the additives. As shown earlier in the DMTA studies, these additives are immiscible, thus resulting in higher set values.

### CONCLUSIONS

The effects of the CI, PF, and PAHY resins, and AO, PS, PP, EPDM rubber, and EVA on the morphology, mechanical, and dynamic mechanical

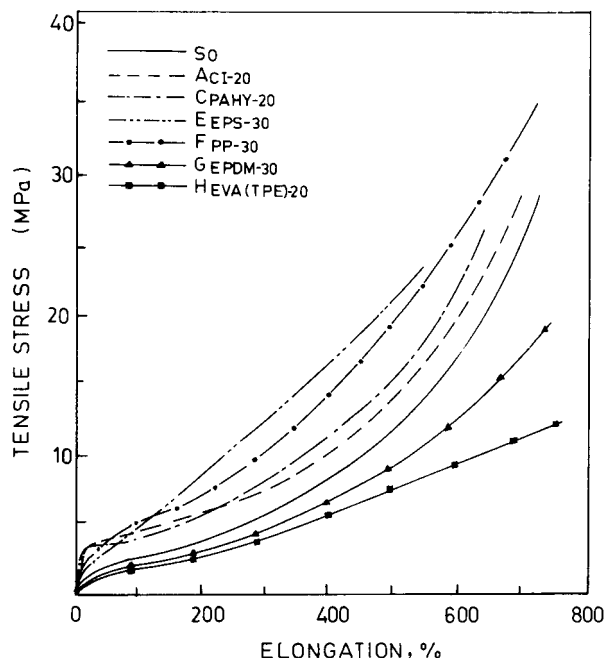


**Figure 6** Stress-strain plots of control and modified SEBS.

properties of SEBS polymer have been investigated. The following conclusions have been made.

1. The CI resin (30 phr) and AO (10 phr) decrease the  $\tan \delta$  peak height of the EB transition but increase the  $\tan \delta$  peak height of the PS transition. The resin increases the EB transition temperature, while AO decreases it. The PS transition temperature, however, decreases in both the cases. As expected, the CI resin enhances the mechanical properties of SEBS, but AO lowers them.
2. PP, of all the additives, have the most prominent effect. It considerably reinforces the mechanical properties of SEBS polymer. This is

because PP forms the continuous matrix while SEBS forms the dispersed phase, as confirmed from SEM photographs. The  $\tan \delta$  peak of SEBS at both the lower and upper transition regions is decreased.

3. Other additives have only a marginal effect. The PF resin, PAHY resin, and PS impart stiffness to SEBS polymer by increasing its modulus only. The tensile strength, however, decreases. EPDM and EVA lower the good mechanical strength of SEBS polymer. The  $\tan \delta$  peak at a low temperature transition decrease in each case, but the one at a high temperature increases.

## REFERENCES

1. N. R. Legge and R. C. Moubay, *Rubber World*, **211**, 43 (1994).
2. G. Holden, *Rubber World*, **208**, 25 (1993).
3. *Handbook of Thermoplastic Elastomers—New Developments and Technology*, A. K. Bhowmick and H. L. Stephens, Eds., Marcel Dekker, New York, 1988.
4. *Block and Graft Copolymerization*, R. J. Ceresa, Vol. I, Wiley, New York, 1973.
5. *Thermoplastic Elastomers—A Comprehensive Review*, N. R. Legge, G. Holden, and H. E. Schroeder, Eds., Hanser, Munich, 1987.
6. J. B. Class, *Rubber Chem. Technol.*, **58**, 973 (1985).
7. B. Ohlsson, H. Hassander, and B. Tornell, *Polym. Eng. Sci.*, **36**, 501 (1996).
8. B. Ohlsson and B. Tornell, *Polym. Eng. Sci.*, **36**, 1547 (1996).
9. C. D. Han, J. Kim, and D. M. Back, *J. Adhes.*, **28**, 201 (1989).
10. C. D. Han, J. Kim, and D. M. Back, *J. Polym. Sci., Part B: Polym. Phys.*, **28**, 315 (1990).
11. C. D. Han and J. Kim, *J. Polym. Sci., Part B: Polym. Phys.*, **26**, 677 (1988).
12. J. B. Class and S. G. Chu, *J. Appl. Polym. Sci.*, **30**, 825 (1985).